

AD-A151 397

IONIC CONDUCTIVITY AND MICROWAVE DIELECTRIC RELAXATION
OF LIASF6 AND LiCl. (U) POLYTECHNIC INST OF NEW YORK
FARMINGDALE DEPT OF CHEMISTRY M DELSIGNORE ET AL.

1/1

UNCLASSIFIED

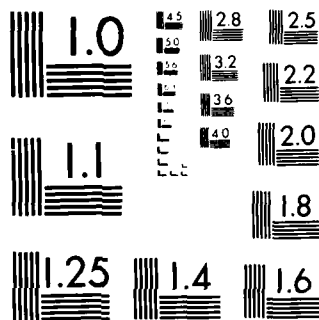
JAN 85 TR-6 ARO-18978. 6-CH DAAG29-82-K-0048 F/G 20/3

NL

END

FILED

DTIC



MICROCOPY RESOLUTION TEST CHART
NATIONAL BUREAU OF STANDARDS-1963-A

AD-A151 397

DTIC FILE COPY

UNCLASSIFIED
SECURITY CLASSIFICATION OF THIS PAGE (When Data Entered)

MASTER COPY - FOR REPRODUCTION PURPOSES

②

REPORT DOCUMENTATION PAGE		READ INSTRUCTIONS BEFORE COMPLETING FORM
1. REPORT NUMBER ARO 18978.6-CH	2. GOVT ACCESSION NO. N/A	3. RECIPIENT'S CATALOG NUMBER N/A
4. TITLE (and Subtitle) Ionic Conductivity and Microwave Dielectric Relaxation of LiAsF₆ and LiClO₄ in Dimethylcarbonate		5. TYPE OF REPORT & PERIOD COVERED Technical
7. AUTHOR(s) Marta Delsignore, Herman Farber and Sergio Petrucci		6. PERFORMING ORG. REPORT NUMBER 6
9. PERFORMING ORGANIZATION NAME AND ADDRESS Polytechnic Institute of New York Department of Chemistry, Long Island Center Route 110, Farmingdale, New York 11735		8. CONTRACT OR GRANT NUMBER(s) DAAG-29-82-K0048
11. CONTROLLING OFFICE NAME AND ADDRESS U. S. Army Research Office Post Office Box 12211 Research Triangle Park, NC 27709		10. PROGRAM ELEMENT, PROJECT, TASK AREA & WORK UNIT NUMBERS
14. MONITORING AGENCY NAME & ADDRESS (if different from Controlling Office)		12. REPORT DATE January 1985
		13. NUMBER OF PAGES
		15. SECURITY CLASS. (of this report) Unclassified
15. DISTRIBUTION STATEMENT (of this report) Approved for public release; distribution unlimited.		15a. DECLASSIFICATION/DOWNGRADING SCHEDULE
17. DISTRIBUTION STATEMENT (of the abstract entered in Block 20, if different from Report) NA		
18. SUPPLEMENTARY NOTES The view, opinions, and/or findings contained in this report are those of the author(s) and should not be construed as an official Department of the Army position, policy, or decision, unless so designated by other documentation.		
19. KEY WORDS (Continue on reverse side if necessary and identify by block number) Electrical conductance, microwave dielectric relaxation, LiAsF₆, Dimethylcarbonate.		
23. ABSTRACT (Continue on reverse side if necessary and identify by block number) Audiofrequency electrical conductivity data are reported in the solvent dimethylcarbonate (DMC) at 25°C in the concentration range 10⁻⁴ to 1M for LiAsF₆ and 10⁻⁴ to 0.3M for LiClO₄. From 10⁻⁴ to ≈ 10⁻²M the data are interpreted by the Fuoss-Kraus triple-ions theory leading to the values of the ion pair formation constant K_p and triple ion formation constant K_T. For the data at higher concentration, it is shown that the change of static permittivity of the solution (due to the presence of solute ion-pairs and other polar species, which increase the polarization of the solution) can account		

DTIC
ELECTE

MAR 19 1985

E

DD FORM 1 JAN 73 1473 EDITION OF 1 NOV 65 IS OBSOLETE

UNCLASSIFIED

85 03 07 021

SECURITY CLASSIFICATION OF THIS PAGE (When Data Entered)

UNCLASSIFIED

SECURITY CLASSIFICATION OF THIS PAGE(When Data Entered)

qualitatively for the behavior of the conductance data and their derivation from the Fuoss-Kraus theory. In other words, these deviations are mostly due to changes in permittivity, not accounted for in the conventional treatment of the data, rather than by the failure of the theory, which is better than recognized so far. Introduction of the quadrupole formation constant is necessary, however, for LiAsF_6 for a more quantitative treatment of the conductance data. Microwave complex permittivities in the concentration range 0.05M to 0.3M, frequency range ≈ 1 to 90 GHz are interpreted by two Debye relaxation processes, one due to the solute and one to the solvent. For LiAsF_6 the Böttcher plot (expressing a quantity related to the change of the relaxation strength ($\epsilon_0 - \epsilon_{\infty}$) with the concentration of electrolyte) is nonlinear with concentration. Correction of the concentration, by postulating the presence of dielectrically apolar dimers linearizes the plot with a quadrupole formation constant of the order of $K_q \approx 50\text{M}^{-1}$, although this figure is very tentative. For LiAsF_6 both rotational relaxation time and the distance separation of the charges as calculated from the apparent dipole moment suggest distances of the order of contact ion pairs. For LiClO_4 no curvature in the Böttcher plot is visible, suggesting that presence of quadrupoles is not significant for this electrolyte in DMC, a notion already reported in the literature. This is somewhat surprising in view of the ionic association constant to pairs K_p , being an order of magnitude larger for LiClO_4 with respect to LiAsF_6 . The distance separation of the charges, as calculated from the apparent dipole moment of LiClO_4 suggests presence of contact species.

Accession For	
NTIS GRA&I	X
DTIC TAB	
Unannounced	
Justification	
By	
Distribution/	
Availability Codes	
Avail and/or	
Dist	Special
A-1	



UNCLASSIFIED

SECURITY CLASSIFICATION OF THIS PAGE(When Data Entered)

Ionic Conductivity and Microwave Dielectric Relaxation
of LiAsF_6 and LiClO_4 in Dimethylcarbonate

by

M. Delsignore,* H. Farber and S. Petrucci

Department of Chemistry and Department of Electrical Engineering

Long Island Center

Polytechnic Institute of New York

Route 110

Farmingdale, NY 11735

ABSTRACT

Audiofrequency electrical conductivity data are reported in the solvent dimethylcarbonate (DMC) at 25°C in the concentration range 10^{-4} to 1M for LiAsF_6 and 10^{-4} to 0.3M for LiClO_4 . From 10^{-4} to $\approx 10^{-2}\text{M}$ the data are interpreted by the Fuoss-Kraus triple-ions theory leading to the values of the ion pair formation constant K_p and triple ion formation constant K_T . For the data at higher concentration, it is shown that the change of static permittivity of the solution (due to the presence of solute ion-pairs and other polar species, which increase the polarization of the solution) can account qualitatively for the behavior of the conductance data and their deviation from the Fuoss-Kraus theory. In other words, these deviations are mostly due to changes in permittivity, not accounted for in the conventional treatment of the data, rather than by the failure of the theory, which is better than recognized so far. Introduc-

* Present address: Colgate-Palmolive Co., Piscataway, New Jersey.

tion of the quadrupole formation constant is necessary, however, for LiAsF_6 for a more quantitative treatment of the conductance data. Microwave complex permittivities in the concentration range 0.05M to 0.3M, frequency range ≈ 1 to 90 GHz are interpreted by two Debye relaxation processes, one due to the solute and one to the solvent. For LiAsF_6 the Böttcher plot, (expressing a quantity related to the change of the relaxation strength $(\epsilon_\infty - \epsilon_{00})$ with the concentration of electrolyte), is nonlinear with the concentration. Correction of the concentration, by postulating the presence of dielectrically apolar dimers linearizes the plot with a quadrupole formation constant of the order of $K_q \approx 50\text{M}^{-1}$, although this figure is very tentative. For LiAsF_6 both rotational relaxation time and the distance separation of the charges as calculated from the apparent dipole moment suggest distances of the order of contact ion pairs. For LiClO_4 no curvature in the Böttcher plot is visible, suggesting that presence of quadrupoles is not significant for this electrolyte in DMC, a notion already reported in the literature. This is somewhat surprising in view of the ionic association constant to pairs K_p , being an order of magnitude larger for LiClO_4 with respect to LiAsF_6 . The distance separation of the charges, as calculated from the apparent dipole moment of LiClO_4 suggests presence of contact species.

Introduction

Research with the electrochemically relevant electrolyte LiAsF_6 has been carried out so far, in this laboratory, in the ethereal solvents 1,2-DME¹ and 2-MethylTHF² of respective permittivities $\epsilon=7.05$ and $\epsilon=6.2$. This electrolyte shows a high solubility ($>1\text{M}$) in the solvent dimethylcarbonate of $\epsilon=3.1^3$. Due to its higher electrolyte strength with respect to LiClO_4 ,⁴ perhaps due to steric and donicity properties of AsF_6^- it was thought quite relevant to carry a parallel investigation of LiAsF_6 and $^{1,2}\text{LiClO}_4$ in DMC also because of the rare chance to extend to high electrolyte concentrations, a study in a medium of such low permittivity. Two experimental methods, audiofrequency electrical conductivity and microwave coaxial and rectangular waveguide reflectometry (leading to the determination of the complex permittivity $\epsilon^*=\epsilon'-j\epsilon''$) have been used at the temperature $t=25^\circ\text{C}$. The present work also extends to higher concentrations of LiClO_4 , some microwave work reported earlier.³

Experimental Part

LiAsF_6 (Agri Chem. Co., Atlanta, Georgia) and LiClO_4 (C. P. Smith Co., Cleveland, Ohio) were dried at 70° in vacuo overnight.¹ Dimethylcarbonate (Aldrich Chemical Co., 99% product) was distilled twice in a ~~cell~~ pyrex Vigreux column without grease on the joints. A portion of DMC was dried over activated 4\AA molecular sieves and distilled over them (about 1/5 of volume of sieves with respect to the liquid). The molecular sieves were dried at $\approx 100^\circ\text{C}$ in vacuo overnight. A conductivity run for LiAsF_6 in DMC distilled over molecular sieves gave same results as for DMC distilled without molecular sieves. For the microwave work, solutions were kept in dessicators. Contact with open atmosphere was kept to a few seconds, namely, the time necessary to fill the cells. The equipment for the conductance work has been extensively described.⁵ The setups for the microwave work has been reported in previous

papers.^{3,6,7} The only change of significance has been in the automation and digitization of data capturing. Specifically, the 1000 Hz modulated signal from the crystal detectors is now fed to a Hewlett-Packard 3408A digital voltmeter which is sensitive to $\pm 1\mu\text{V}$. The meter is part of a loop comprising a Hewlett-Packard 41CV calculator a HP-82160A-1L interface and a HP82162A thermal printer. The ac modulated voltage is transmitted to the calculator upon pressing a command that induces the calculator to "listen" to the voltmeter. The calculator in turn "talks" to the printer giving the decimal log of the digitized voltage which gets hard copied. The micrometric measurements of the reflector have also been motorized with the result that the system is a semiautomatic reflectometer recording the db vs. distance of the reflector receding from the mica window holding the liquid at the bottom of the coaxial line (1-4 GHz) or of various waveguides (8-90 GHz).

Results and Discussion

a) Electrical Conductance

Table I reports the equivalent electrical conductivities $\Lambda (\Omega^{-1}\text{cm}^2\text{eq}^{-1})$ and the molar concentration c (M) for LiAsF_6 in DMC at 25°C . Four runs were performed with two conductance cells of cell constant $K_c=0.1156\text{cm}^{-1}$ and $K_c=0.2794\text{cm}^{-1}$. This last cell was used for Run #4 at $c > 0.5\text{M}$. The cell of lower constant was recalibrated with recrystallized KCl dissolved in water, measuring the cell impedance in the frequency range 1000, 5000 Hz and using the Fuoss et al. equation⁸ for the cell calibration:

$$\Lambda = 140.93 - 94.65c^{1/2} + 58.74 \log c + 108.4c.$$

The result over five solutions was

$$K_c = (0.1156 \pm 0.0004)\text{cm}^{-1}$$

Fig. 1 shows the same data in the form of $\log_{10}\Lambda$ vs. $\log_{10}c$. A dramatic

change, over several order of magnitudes for Λ , changing with concentration, takes place. Clearly, at $\approx 1M$ we have a conductivity comparable to the one of $LiAsF_6$ in DME at $c \approx 10^{-4}M$, a not too surprising event if one realizes that the permittivity of the solution has increased dramatically from $\epsilon=3.1$, the value of the solvent, as shown below. In the range of electrolyte concentration 10^{-4} to $10^{-2}M$, the classical Fuoss-Kraus theory for triple-ion formation⁹ reads

$$\Lambda g(c) \sqrt{c} = \frac{\Lambda_o}{\sqrt{K_p}} + \frac{\Lambda_o^2 K_T}{\sqrt{K_p}} \left(1 - \frac{\Lambda}{\Lambda_o}\right) c \quad (I)$$

with

$$g(c) = \frac{\exp\left(-2.303 \frac{\beta'}{\Lambda_o^{1/2}} \sqrt{c} \Lambda\right)}{\left(1 - \frac{S}{\Lambda_o^{3/2}} \sqrt{c} \Lambda\right) \left(1 - \frac{\Lambda}{\Lambda_o}\right)^{1/2}}$$

where β' is the Debye-Huckel activity coefficient term

$$\beta' = \frac{1.8247 \times 10^6}{(\epsilon T)^{3/2}}$$

and

$$S = \alpha \Lambda_o + \beta = \frac{0.8204 \times 10^6}{(\epsilon T)^{3/2}} \Lambda_o + \frac{82.501}{\eta (\epsilon T)^{1/2}}$$

is the Onsager conductance term. We have used $\epsilon = 3.12$, $\eta = 0.00585$, and $\Lambda_o(LiAsF_6) = 97.4$, $\Omega^{-1}cm^2eq^{-1}$, based on $\Lambda_o = 22.53$ in propylenecarbonate, $\eta = 0.0253p$ and the Walden rule. The results, applying Eq. 1 to the data, are determination coefficient $r^2 = 0.988$, Intercept = 1.033×10^{-4} , Slope = 0.0306 , from which $K_p = 8.9 \times 10^{11} M^{-1}$ and $K_T = 445 M^{-1}$, having chosen the arbitrary position $\Lambda_T^o = \frac{2}{3} \Lambda_o$ as done previously. Fig. 2 reports an illustration of function (I) for the present data.

Figs. 3a shows the $\log_{10}\Lambda$ data for LiClO_4 in DMC at 25° , plotted vs. $\log_{10}c$. Table I reports the Λ and c data for the two runs performed for LiClO_4 in DMC at 25°C . One can see immediately by comparing Figs. 1 and 3 that the equivalent conductance of LiClO_4 is one order of magnitude lower than that of LiAsF_6 at the same total concentration. Application of Eq. (I) to the data at $c < 10^{-2}\text{M}$ for LiClO_4 is shown in Fig. 3b. Linear regressions of $\Lambda g(c)\sqrt{c}$ vs. $c(1 - \frac{\Lambda}{\Lambda_o})$ gives $r^2 = 0.993$, Intercept = 0.3937×10^{-4} , Slope = 0.0110, from which $K_p = 8.6 \times 10^{12}\text{M}^{-1}$ and $K_T = 418\text{M}^{-1}$, with $\Lambda_o^T = \frac{2}{3}\Lambda_o$, as done above.

For the above calculation we have used $\Lambda_{\text{LiClO}_4}^o = 115.7\Omega^{-1}\text{cm}^2\text{eq}^{-1}$ in DMC, based on Walden's rule and the results for LiClO_4 in propylenecarbonate $\Lambda_o = 26.75\Omega^{-1}\text{cm}^2\text{eq}^{-1}$ and $\eta = 0.0253\text{p}$. By using for both LiAsF_6 and LiClO_4 the data for Λ_o in propylenecarbonate, having the same $\begin{smallmatrix} \text{O} \\ \diagup \text{C} = \text{O} \end{smallmatrix}$ polar group as DMC, it is hoped to achieve a reasonable validity of Walden's rule.

An attempt has been made at this point to see whether the positive deviation of the Fuoss Kraus $\Lambda g(c)\sqrt{c}$ vs. $(1 - \Lambda/\Lambda_o)c$ plot, a trend observed before^{1,2} for concentrations higher than $c \approx 10^{-2}\text{M}$ was due to causes other than the ionic strength. It is our contention that the latter is quite low in DMC and that the apparent failure of the theory to represent the data at $c > 10^{-2}\text{M}$ is in part due to the inappropriate permittivities and viscosities used in the theoretical expressions. From the microwave portion of the work, we have fitted the static permittivities ϵ for LiAsF_6 solutions to the electrolyte concentration c by a cubic polynomial equation which gives by nonlinear regressions

$$r^2 = 0.9993 \quad \epsilon = 3.11 + 27.479c - 110.340c^2 + 199.25c^3 \quad (\text{II})$$

valid up to $c = 0.25\text{M}$. In the same concentration range the solution densities

are given by

$$r^2 = 0.99994 \quad \rho = 1.063 + 0.1879c - 0.2185c^2 + 0.1655c^3$$

valid within ± 0.001 g/cm³. It is noteworthy to emphasize the point raised above that at 0.25M $\epsilon = 6.20$ instead of $\epsilon = 3.11$, the solvent value. We have then decided to take the variation into account in dealing with the Fuoss-Kraus theory, a concept already expressed years ago by E.A.S. Cavell¹¹. In addition, we have corrected the viscosities by the presence of the electrolyte LiAsF₆ by the Einstein equation, as suggested by Fuoss¹²:

$$\eta^E = \eta_o \left[1 + \frac{5}{2} \phi \right] = \eta_o [1 + Fc] \quad (\text{III})$$

where ϕ is the volume fraction $\phi = \frac{(4\pi R^3/3)Lc}{1000} = \frac{2}{5}Fc$ and $F = 6.308 \times 10^{21} R^3$.

R , the radius of the pair (taken as a sphere) has been estimated by the Debye expression $\tau = \frac{4\pi R^3}{kT} \eta$, $\tau = (2\pi f)^{-1}$ neglecting differences between the decay of the polarization τ_D and the real molecular relaxation time τ that enter the Debye equation. Similarly, $\eta \approx \eta_o = 0.00585$ poise has been retained. With $\bar{f} = 1.7 \times 10^9$ Hz, it results $R = 3.7 \times 10^{-8}$ a value comparable with the sum of the crystallographic radii for LiAsF₆ giving $R_{\text{cry}} = 4.4 \times 10^{-8}$ cm. One should also point out that we are in complete agreement with Fuoss¹² in that Eq. (III) ought to be used instead of the experimental viscosities. The latter incorporates the Falkenhagen term S_η

$$\eta = \eta_o (1 + S_\eta \sqrt{c} + Fc)$$

expressing the existing velocity gradient in the solution which are absent in the conductance experiment where the solution is at rest as a whole. It results for LiAsF₆ in DMC that $F = 0.3$ and $\eta^E = \eta_o (1 + 0.3c)$. By the aid of Eqs. II and III, we have calculated Eq. I, namely, the $g(c)$ term corrected by $\epsilon(c)$ and η^E . The data for LiAsF₆ in DMC are reported in Fig. 4. We have then tried to cal-

culate the right side of Eq. (I) from theory, using the expressions by Fuoss-Jagodzinski¹⁴

$$K_p = K_{FJ} = \frac{4\pi L a^3}{3000} e^{-1/2} e^b \quad (IV)$$

$$K_T = K_{FJ}^T = \frac{\pi L a^3}{1000} e^{-3/2} e^{b/2}$$

Specifically, we have equated Eqs.(IV) to the values of K_p and of K_T for $LiAsF_6$ found experimentally in the low concentration range, namely, $K_p=8.9 \times 10^{11} M^{-1}$ and $K_T=445 M^{-1}$ obtaining (with $\epsilon=3.12$) $a=6.3 \times 10^{-8} cm$ and $a_T=16.4 \times 10^{-8} cm$. Without assigning to these parameters physical significance, we have used these numerical values to calculate Eqs. (IV) at all the concentrations using Eq. (II) to evaluate ϵ .

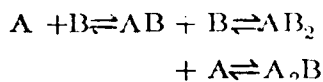
The results for $LiAsF_6$ solutions in DMC are reported in Fig. 4 together with the calculated $[\Lambda \sqrt{c} g(c)]_{calc}$ according to the right side of Eq. (I) and also by using $\Lambda_T^0 = \frac{1}{3} \Lambda_0$ as in the original version of the triple-ion theory³. In Fig. 4 the solid lines represent these calculated values showing a qualitative trend following the data at variance with the original Fuoss-Kraus theory using $\epsilon = 3.12$ and $\eta = 0.00585$. The introduction of $\epsilon(c)$ and η^E seems, however, to have overcorrected the $\Lambda g(s) \sqrt{c}$ data. The results from the microwave data, shown below for $LiAsF_6$ in DMC, indicate that the ion pairs are not the only complex species present. The Böttcher plot shows a strong concave down curvature indicating lack of proportionality of the relaxation strength $\epsilon_0 - \epsilon_\infty$, with the total concentration. This, in turn, suggests that the polarization of the solution is not proportional to c and that the total concentration is different from c_p , the ion pair concentration. The situation is corrected by the introduction of a quadrupole equilibrium with $K_q \sim 50 M^{-1}$.

We have applied the same criterion to the conductance data of $LiAsF_6$ in

DMC, expressing the total concentration by the two major species present (free ions and triple ions are in minor quantities)

$$c = (AB) + 2(\Lambda_2B_2) = c_p + 2c_p^2K_q$$

and using c_p rather than c in the Fuoss-Kraus definition



with $(A)=(B)=\alpha c_p$; $(AB) = c_p(1 - \alpha - 3\alpha_T)$; $(AB_2) = (\Lambda_2B) = \alpha_T c_p$ leading to the usual expression

$$\Lambda_o g(c) \sqrt{c_p} = \frac{\Lambda_o}{\sqrt{K_p}} + \frac{\Lambda_o^T K_T}{\sqrt{K_p}} \left(1 - \frac{\Lambda}{\Lambda_o}\right) c_p \quad (V)$$

which differs from Eq. (I) only by the presence of c_p instead of c . Fig. 5 reports the left and right side of equation (V) depicted, the former by the experimental point, the latter by the solid line. Although the data for $\Lambda_o^T = \frac{1}{3}\Lambda_o$ are overcorrected in the lower portion of the curve and undercorrected in the upper portion, the general qualitative trend is followed up to $c \approx 0.1M$, a large improvement over the original calculations using $\epsilon = 3.12$ and $\eta = 0.00585$, the solvent properties.

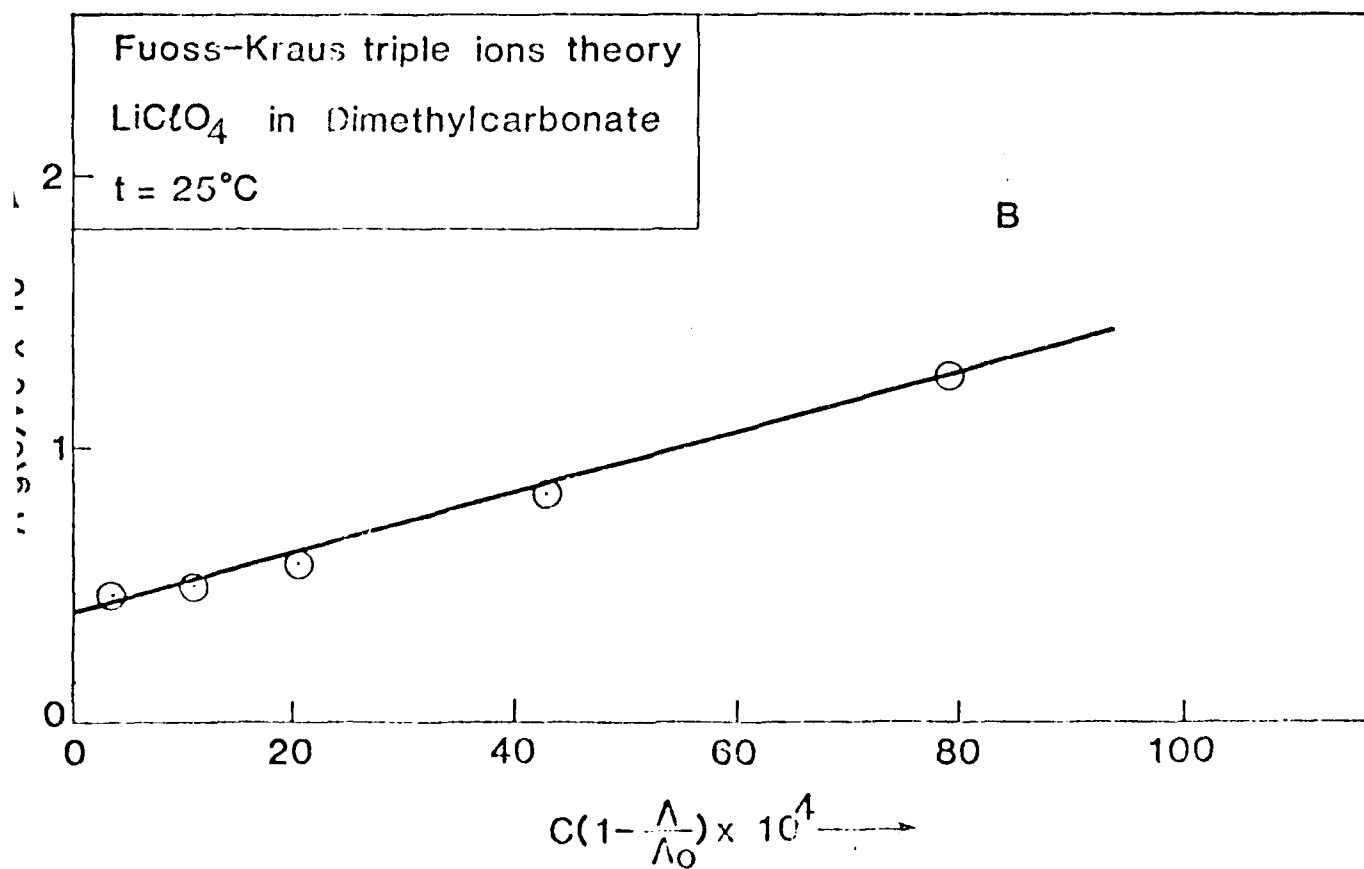
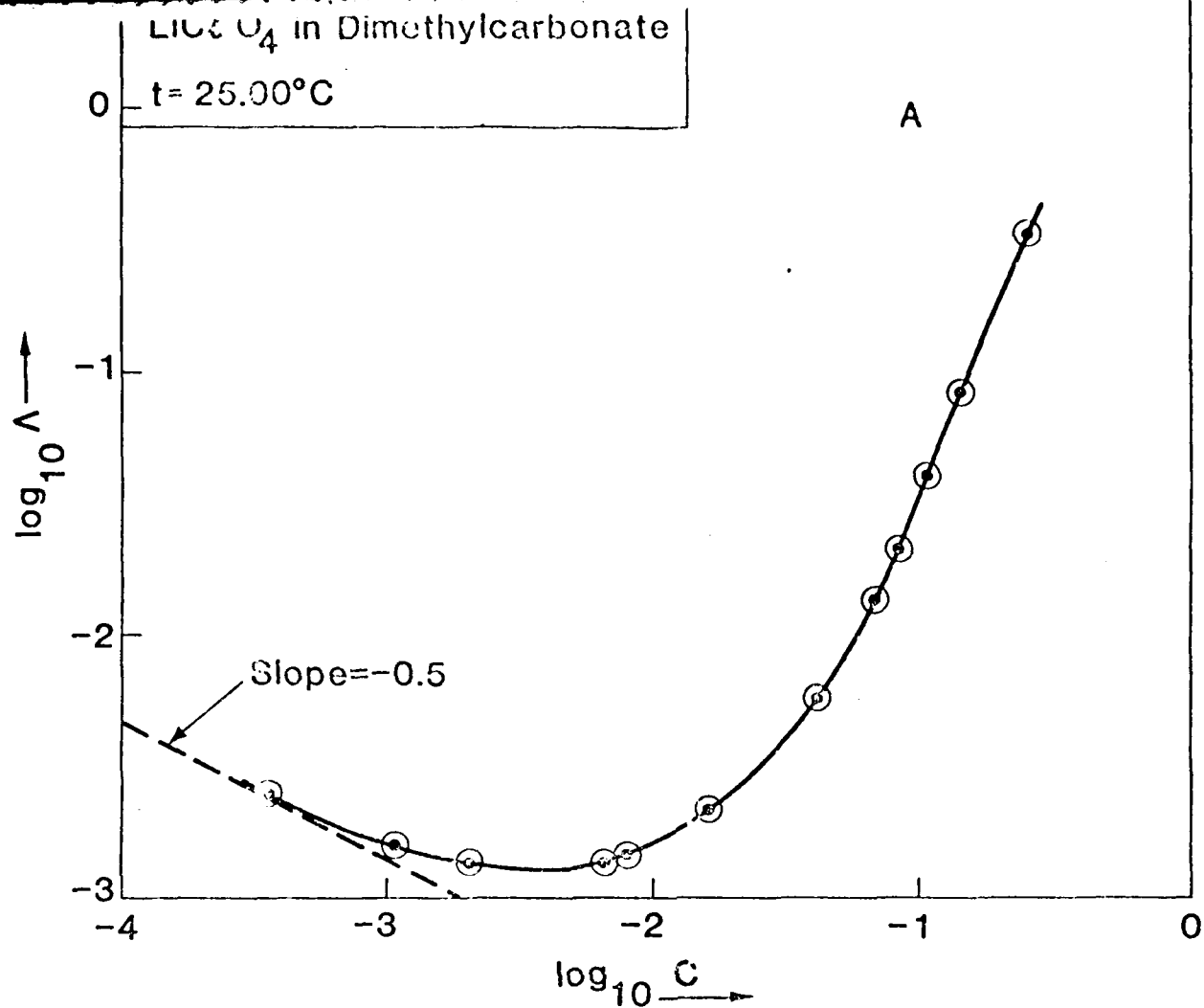
The same sequence of calculations has been applied to the $LiClO_4$ data. The permittivity is expressible in terms of the concentration of $LiClO_4$ by the expression $\epsilon = 3.12 + 7.833c + 47.228c^2 - 125.61c^3$ with $r^2 = 1.0000$. The density of the solutions can be expressed by the relation $\rho = 1.063 - 0.024856m + 1.0607m^2 - 2.4134m^3$ with m the molality of the solutions and $r^2 = 0.99993$. The average lower decay time of the polarization of the solutions taken to be approximately equal to the relaxation time $\tau = (2\pi f)^{-1} = (2\pi \times 1.3 \times 10^9)^{-1} = 122.4 \times 10^{-12}$ seconds which, by the aid of the Debye expression $\tau = (4\pi R^3/kT)\eta$ gives $R = 4.09 \times 10^{-8} cm$. This value intro-

duced into the Einstein relation $\phi = (4\pi R^3/3) Lc/1000 = (2/5)Fc$ gives $F = 0.43$ and $\eta^E = \eta_0 (1 + 0.43c)$.

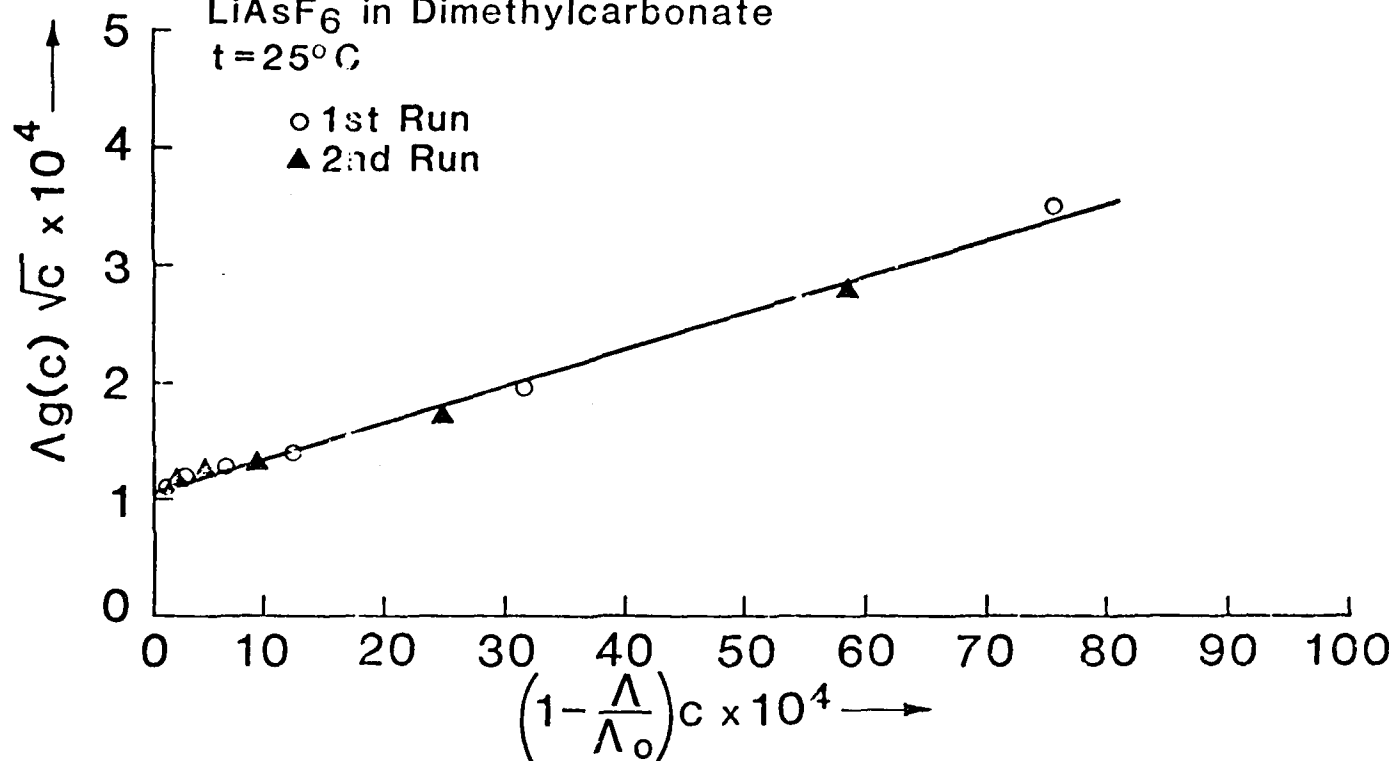
The calculation has been then applied using equation (I) as for the case of the LiAsF_6 data, using the $\epsilon(c)$ and η^E data. The results of this calculation are depicted in Fig. 6 where the solid lines correspond to the theoretical $\Lambda g(c)\sqrt{c}$, calculated by the aid of equations (V) $\Lambda_o^T = \frac{2}{3}\Lambda_o$ and $\Lambda_o^T = \frac{1}{3}\Lambda_o$. The values of $a = 5.8 \times 10^{-8} \text{ cm}$ and $a_T = 16.8 \times 10^{-8} \text{ cm}$ have been used based on the fit of the experimental $K_p = 8.6 \times 10^{12} \text{ M}^{-1}$ $K_T = 418 \text{ M}^{-1}$ from the low concentration data. From Fig. 6 the same consideration as for LiAsF_6 hold, namely, the agreement of the calculated and experimental data although qualitative, encompasses a larger concentration range than in the original theory using $\epsilon = 3.12$ and $\eta = 0.00585\rho$.

The difference from the LiAsF_6 case is that there is no need of introducing a quadrupole constant, as evidenced also by the microwave data showing no evidence of quadrupole complexation for LiClO_4 , the Böttcher plot being linear. In the above calculation of $\Lambda g(c)\sqrt{c}$ the best fit is obtained by the position $\Lambda_o^T = \frac{1}{3}\Lambda_o$ as in the original Fuoss-Kraus theory.⁹ One could surmise that by adjusting K_p , K_T , and K_q (for LiAsF_6) the fit may become better. Here, however, we wish only to stress the concept that by using the information from the microwave experiments (that the permittivity of the solution changes) and by correcting viscosities, a significant improvement over the concentration range usable by the conductance theory can be obtained.

In other words, at very low permittivities, where very few ions are present, the failure of the theory is not due to ionic strength effects, but rather to the neglect of the effect of the presence of large quantities of neutral species and their altering the permittivity ϵ and viscosity η . Improvements on the theory



Fuoss - Kraus triple ions theory
LiAsF₆ in Dimethylcarbonate
t = 25°C



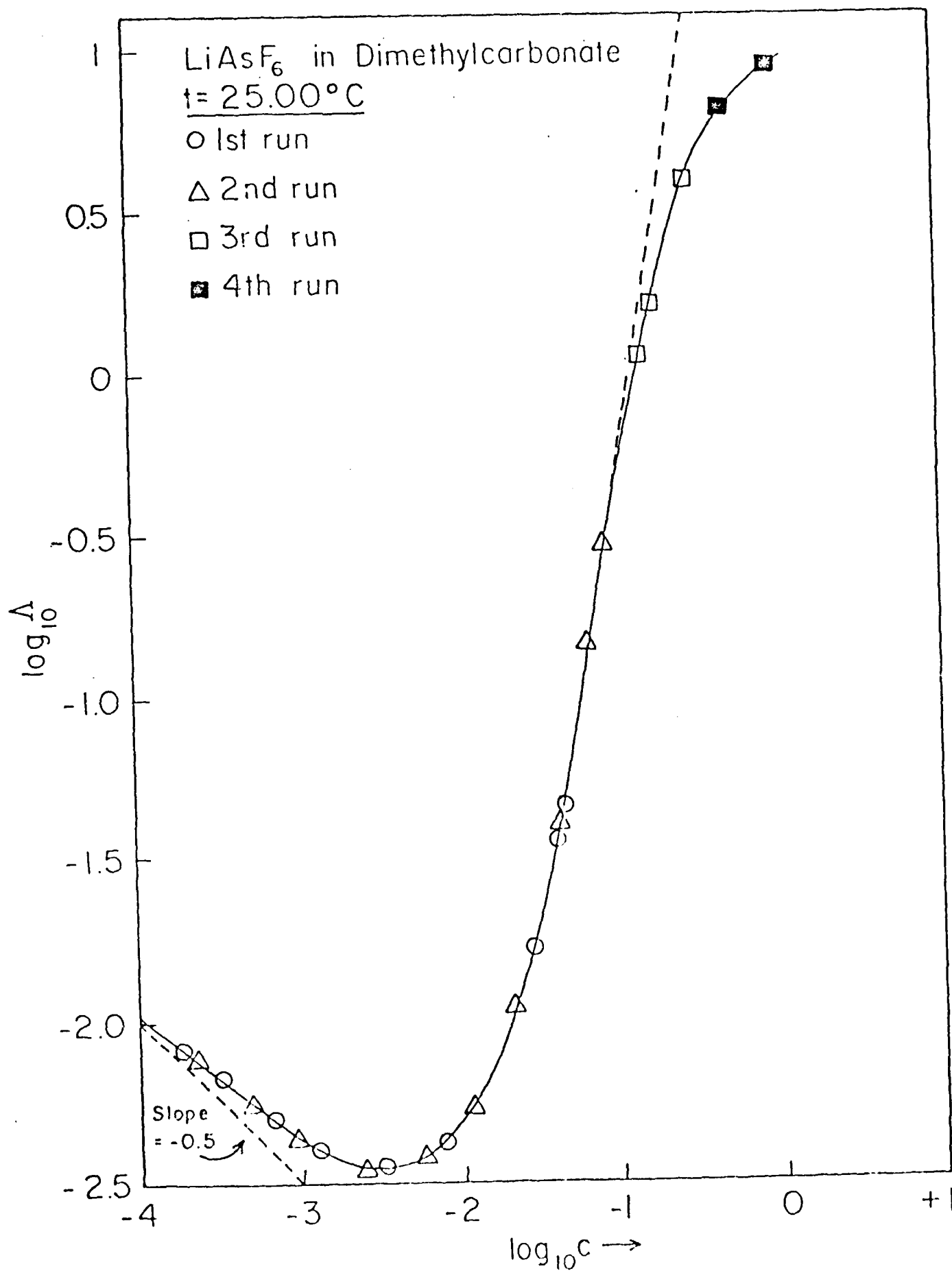


Fig. 9 Böttcher function $\phi(\epsilon) = (\epsilon_o - \epsilon_{oo1}) \frac{2\epsilon_o + 1}{3\epsilon_o}$ vs. c and vs.

$$c_p = \frac{-1 + \sqrt{8K_q c + 1}}{4K_q}$$

for LiAsF_6 in DMC at $t = 25^\circ\text{C}$. K_q is the dimerization constant for ion pairs to quadrupoles (or dimers).

Fig. 10 Böttcher function $\phi(\epsilon) = (\epsilon_o - \epsilon_{oo1}) \frac{2\epsilon_o + 1}{3\epsilon_o}$ vs. c for LiClO_4 in

DMC at $t = 25^\circ\text{C}$.

List of Figures

- Fig. 1 $\log_{10}\Lambda$ vs. $\log_{10}c$ for LiAsF_6 in DMC at 25°C . Λ is the equivalent conductivity, c is the molar concentration.
- Fig. 2 $\Lambda g(c)\sqrt{c}$ vs. $(1 - \frac{\Lambda}{\Lambda_0})c$ for LiAsF_6 in DMC at $c \leq 0.01\text{M}$.
- Fig. 3a $\log_{10}\Lambda$ vs. $\log_{10}c$ for DMC at $t = 25^\circ\text{C}$.
- Fig. 3b $\Lambda g(c)\sqrt{c}$ vs. $(1 - \frac{\Lambda}{\Lambda_0})c$ for LiClO_4 in DMC at $c \leq 0.01\text{M}$.
- Fig. 4 $\Lambda g(c)\sqrt{c}$ vs. $(1 - \frac{\Lambda}{\Lambda_0})c$ for LiAsF_6 in DMC at $c \leq 0.07\text{M}$. $g(c)$ has been calculated with $\epsilon(c)$ and η^E (see text).
- Fig. 5 $\Lambda g(c_p)\sqrt{c_p}$ vs. $(1 - \frac{\Lambda}{\Lambda_0})c_p$ for LiAsF_6 in DMC at 25°C . c_p has been calculated from the expression $c = c_p + 2K_q c_p^2$ with $K_q = 50\text{M}^{-1}$. Also $\epsilon(c)$ and η^E have been used for the calculation of $g(c_p)$.
- Fig. 6 $\Lambda g(c)\sqrt{c}$ vs. $(1 - \frac{\Lambda}{\Lambda_0})c$ for LiClO_4 in DMC at $c \leq 0.07\text{M}$. $g(c)$ has been calculated with $\epsilon(c)$ and η^E (see text).
- Fig. 7a ϵ' vs. f and $\epsilon_d'' = (\epsilon'' - \epsilon_x'')$ vs. f for LiAsF_6 0.25M .
- Fig. 7b Cole-Cole plot: $\epsilon_d'' = (\epsilon'' - \epsilon_x'')$ vs. ϵ' for LiAsF_6 0.25M in DMC.
- Fig. 8a ϵ' vs. f and ϵ'' vs. f for LiAsF_6 0.15M in DMC; $t=25^\circ\text{C}$.
- Fig. 8b Cole-Cole plot of $\epsilon_d'' = (\epsilon'' - \epsilon_x'')$ vs. ϵ' for LiAsF_6 0.15M in DMC.

TABLE II

Dielectric Relaxation Parameters and Electrical Conductivity X for LiAsF_6 and LiClO_4 in Dimethylcarbonate at 25°C at the Concentrations Investigated.

 LiAsF_6

c	ϵ_0	$\epsilon_{\infty 1}$	$\epsilon_{\infty 2}$	f_1 (GHz)	f_2 (GHz)	X ($\Omega^{-1} \text{cm}^{-1}$)	$ \overline{\Delta \epsilon'} ^a$	$ \overline{\Delta \epsilon''} ^a$
0.25	6.20	3.50	2.50	1.6	22	7.38×10^{-4}	0.095	0.06
0.15	5.40	3.40	2.45	1.8	22	1.66×10^{-4}	0.04	0.05
0.10	5.00	3.30	2.40	1.6	22	3.98×10^{-5}	0.08	0.05
0.05	4.20	3.20	2.40	1.8	22	2.94×10^{-6}	0.04	0.02

 LiClO_4

0.29	6.30	3.40	2.45	1.4	22	1.24×10^{-4}	0.026	0.041
0.19	5.50	3.35	2.45	1.3	22	3.22×10^{-5}	0.053	0.047
0.10 ^b	4.25	3.30	2.40	1.2	18	3.46×10^{-6}	0.64	0.28
0 ^b		3.12	2.35	--	22	----	0.35	0.22

^a $|\overline{\Delta \epsilon'}|$ and $|\overline{\Delta \epsilon''}|$ the absolute average deviations ($\epsilon'^{\text{calc}} - \epsilon'^{\text{exp}}$) and ($\epsilon''^{\text{calc}} - \epsilon''^{\text{exp}}$).

^b Saar, D., Brauner, J., Farber, H., Petrucci, S., J. Phys. Chem. 82 (1978) 5451.

TABLE I (Continued)

Equivalent Conductance Λ and Molar Concentration c for LiClO_4
in Dimethylcarbonate; $t = 25^\circ\text{C}$.

	$c \times 10^4$ (M)	Λ ($\Omega^{-1}\text{cm}^2\text{eq}^{-1}$)
Run No. 1 ^{a)}	3.5683	0.0025203
	10.720	0.0015583
	20.323	0.0013282
	42.937	0.0013181
	78.760	0.0014885
	159.865	0.0021431
	412.97	0.0058785
	696.65	0.013938
	863.82	0.021501
	1059.4	0.041264
Run No. 2	1417.4	0.084089
	2488.3	0.3368

^{a)} Both runs were performed with a cell of constant $K_c = 0.1156 \text{ cm}^{-1}$.

TABLE I

Equivalent Conductance Λ and Molar Concentration c for
 LiAsF_6 in Dimethylcarbonate; $t = 25^\circ\text{C}$

<u>Run No. 1</u>		<u>Run No. 2</u>	
$c \times 10^4$ (M)	Λ ($\Omega^{-1} \text{cm}^2 \text{eq}^{-1}$)	$c \times 10^4$ (M)	Λ ($\Omega^{-1} \text{cm}^2 \text{eq}^{-1}$)
1.8881	0.008235	2.2480	0.007718
3.2683	0.006724	4.9147	0.005702
6.669	0.005031	9.2272	0.004404
12.282	0.004052	24.829	0.003526
31.446	0.003626	58.403	0.003832
75.513	0.004278	113.06	0.005421
142.59	0.006703	216.50	0.01102
281.56	0.016853	427.08	0.03960
412.96	0.036562	692.08	0.1442
450.84	0.045138	884.22	0.2935
<u>Run No. 3</u>		<u>Run No. 4</u>	
1511.9	1.1488	5127	6.8609
1807.4	1.6670	10,090	9.002
3110.5	3.9865		

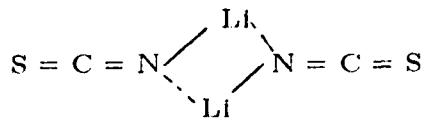
Runs 1, 2, and 3 were performed with a cell of constant $K_c = 0.1156 \text{ cm}^{-1}$,
 Run 4 with a cell of constant $K_c = 0.2794 \text{ cm}^{-1}$.

16. Menard, D., Chabanel, M., J. Phys. Chem (1975) 79, 1081.
17. Saar, D. Brauner, J., Farber, H., Petrucci, S., J. Phys. Chem. (1978) 82, 1943.
18. Paoli, M., Lucon, M., Chabanel, M., Spectrochimica Acta (1979) 354, 593.

References

1. Farber, H., Irish, D. E., Petrucci, S., J. Phys. Chem. (1983) 87, 3515.
2. Delsignore, M., Maaser, H. E., Petrucci, S., J. Phys. Chem. (1984) 88, 2405.
3. Saar, D., Brauner, J., Farber, H., Petrucci, S., J. Phys. Chem. (1972) 82, 545.
4. Maaser, H. E., Delsignore, M., Newstein, M., Petrucci, S., J. Phys. Chem. (1984) 88, 5100.
5. Petrucci, S., Hemmes, P., Battistini, M., J. Am. Chem. Soc. (1967) 89, 5552.
6. Farber, H., Petrucci, S., J. Phys. Chem. (1975) 79, 1221.
7. Farber, H., Petrucci, S., J. Phys. Chem. (1981) 85, 1396.
8. Lind, J. E., Zwolenik, J. J., Fuoss, R. M., J. Am. Chem. Soc. (1959) 81, 1557.
9. Fuoss, R. M., Kraus, C. A., J. Am. Chem. Soc. (1933) 55, 2387.
10. Salomon, M., Plichta, E. J., Electrochim. Acta. 29 (1984) 731.
11. Cavell, E. A. S., Knight, P. C., Zeit. für Physik. Chem. N. F. (1968) 57, 3.
12. Fuoss, R. M., Accascina, F., "Electrolytic Conductance" Intersci. N.Y., 1959, page 234.
13. Falkenhagen, H., Dole, M., Z. Physik. Chem. (1929) 6, 159; Falkenhagen, H., Physik. Z. (1931) 32, 365, 745.
14. Jagodzinski, P., Petrucci, S., J. Phys. Chem. (1974) 78, 917.
15. Böttcher, C. F., "Theory of Electrical Polarization," Elsevier Amsterdam, 1973.

ence of a centrosymmetrical quadrupole¹⁸



which by symmetry would have a zero dipole moment in accord to our contention for LiSCN in DMC and DEC.

Figure 10 reports the Böttcher plot, according to Eq. (VII) for the dielectric data of LiClO₄ in DMC. Linear regressions giving 50% statistical weight to the origin gives $r^2 = 0.995$ slope = 7.413 from which one calculates the apparent dipole moment $\mu = 11.0 \times 10^{-18}$ esu cm. By taking a rigid sphere model (consistent with having neglected the polarization-reaction field term $(1-\alpha f)^2$ gives $\mu = ae$ and $a = 2.3 \times 10^{-8}$ cm giving a strong indication of contact species for LiClO₄.

It is noteworthy that no curvature of the Böttcher plot is visible, at variance with the case of LiAsF₆ in DMC, indicating apparent absence of quadrupoles for LiClO₄ in DMC. This is somewhat surprising in view of $K_p(\text{LiClO}_4) > K_p(\text{LiAsF}_6)$. One could, however, invoke the smaller dipole moment of LiClO₄ with respect to LiAsF₆, hence the smaller dipole-dipole energy $\mu_1 \mu_2 \cos \theta / \epsilon r^3$ (with θ the angle of mutual orientation) as the reason for the undetectable K_q for the case of LiClO₄.

$r^2 = 0.990$ Int = 0.017, slope = 42.89 for $K_q = 50 \text{ M}^{-1}$. One ought to add, however, that the optimum fit is rather insensitive on K_q , a value of $K_q = 30 \text{ M}^{-1}$ giving almost as good a result as $K_q = 50 \text{ M}^{-1}$. Using $K_q = 50 \text{ M}^{-1}$, the apparent dipole moment results $\mu = 26.5 \times 10^{-18} \text{ esu cm}$, namely, $a_\mu = 5.5 \times 10^{-8} \text{ cm}$, taking a rigid sphere model $\mu = ae$ for LiAsF_6 in DMC. With $K_q = 30 \text{ M}^{-1}$, $r^2 = 0.990$, Int = 0.063, $S = 33.35$, $\mu = 23.3 \times 10^{-18} \text{ esu cm}$ and $a_\mu = 4.9 \times 10^{-8} \text{ cm}$

In either case one may be led to the conclusion that a_μ is of the order of magnitude of the sum of the crystallographic radii. Values for the dimerization constants have been calculated by Chabanel et al.,¹⁶ from static dielectric data for LiBr, LiSCN and AgClO_4 . The calculation was based on assuming that the static dielectric increments over the solvent were due to *both* monomer pairs and dimers or quadrupoles

$$\Delta\epsilon = \delta_1(AB) + \delta_2(A_2B_2)$$

implying that the quadrupoles are polar and that $\delta_2 \neq 0$. In fact, it was reported that $\delta_2 = 1.8$ for LiBr, $\delta_2 = 10.8$ for LiSCN and $\delta_2 = 8.6$ for AgClO_4 giving quadrupole constants $K_q(\text{LiBr}) = 90 \text{ M}^{-1}$, $K_q(\text{LiSCN}) = 20 \text{ M}^{-1}$ and $K_q(\text{AgClO}_4) = 45 \text{ M}^{-1}$. For LiClO_4 the effect of quadrupoles was undetectable. Later, however, it was found¹⁷ that for both dimethylcarbonate and diethylcarbonate solvents, for LiSCN and LiClO_4 , the microwave complex permittivity data extrapolated to static values ϵ_0 's comparable with the data by Chabanel et al. As the microwave data were interpretable by a single Debye relaxation which was assigned to the rotation of only polar ion-pairs, one had to conclude¹⁷ that the dimers were apolar. Hence, the assumptions on the δ_2 's made by Chabanel and the calculated K_q 's had to be incorrect. It is also noteworthy that IR spectra in ethers in the 2040cm^{-1} range indicated the pres-

where $|\Delta\epsilon'| = |\epsilon'(\text{calc}) - \epsilon'(\text{exp})|$ and $|\Delta\epsilon''| = |\epsilon''(\text{calc}) - \epsilon''(\text{exp})|$ are the absolute values of the deviations.³ We have already shown in the conductance section dealing with the LiAsF_6 data that the value of α obtained from the decay time of the polarization τ is comparable to the sum of the crystallographic radii, at least as an order of magnitude. In order to gain more structural information on the system, we have plotted the Böttcher function¹⁵

$$\epsilon_o - \epsilon_{oo_1} = \frac{4\pi L \epsilon \times 10^{-3}}{(1 - \alpha f)^2} \frac{\mu^2}{3kT} \frac{3\epsilon_o}{2\epsilon_o + 1} \quad (\text{VII})$$

in the form $(\epsilon_o - \epsilon_{oo_1}) \frac{2\epsilon_o + 1}{3\epsilon_o}$ vs. c for LiAsF_6 in DMC. Neglecting the polarizability α , reactor field factor of term $(1 - \alpha f)^2$ of the order of unity, one would expect a straight line. In fact in Fig. 9 one may see a strong concave down curvature.* This behavior becomes obvious if one realizes that in DMC one ought to expect much higher dimerization of pairs than in the DME and 2MTHF ethers studied so far. This is because of the lower permittivity of DMC.

If one accepts the idea that polar dimers are formed, ruled by the equilibrium $2AB \rightleftharpoons (A_2B_2)$ and $K_q = \frac{(A_2B_2)}{(AB)^2}$ then by combining the expressions

$$C = (AB) + 2(A_2B_2)$$

$$K_q = (A_2B_2)/(AB)^2$$

$c_p = AB$ can be calculated for tentative values of K_q . Linear regressions of $\phi(c)$ vs. c_p should give the best straight line for the best K_q . The calculation has been done and shown in Fig. 9 leading to

* Nonlinear regression of

$$\phi(c) = (\epsilon_o - \epsilon_{oo_1}) \frac{2\epsilon_o + 1}{3\epsilon_o}$$

vs. c gives $r^2 = 0.9998$

$$\phi(c) = -0.002 + 19.534c - 91.273c^2 + 177.023c^3$$

giving 50% statistical weight to the origin.

will have to be made by trying to incorporate these changes, nowadays measurable by modern tools as microwave spectrometry for ϵ , rather than trying to improve on the mathematical treatment. This to date, expressed by the Onsager-Fuoss-Kraus various editions of the theory¹² remains an unsurpassed legacy of ingenuity, elegance and rigor.

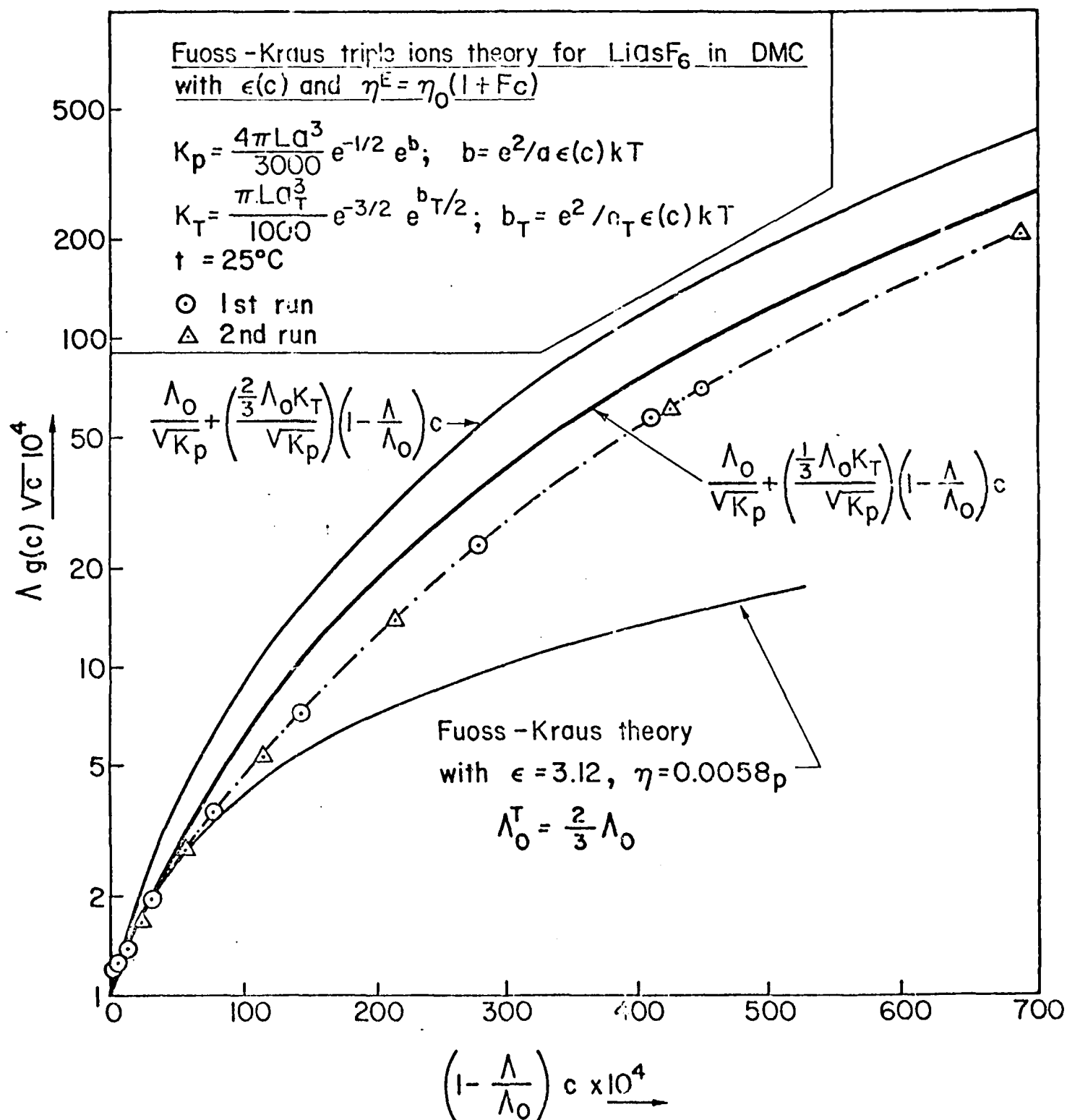
b) Microwave Complex Permittivities

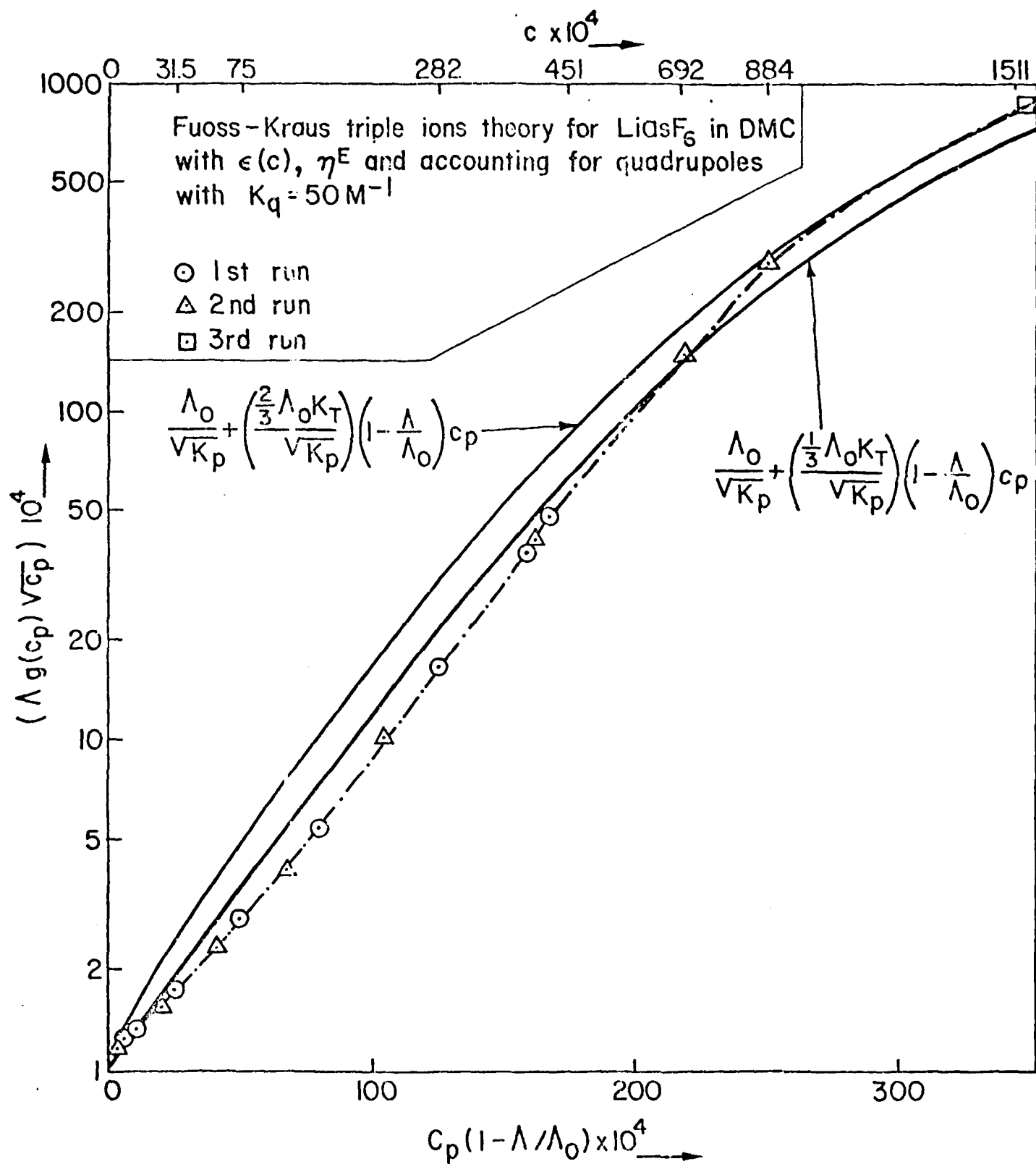
Figures 7 and 8 show representative plots of the coefficient of the real part ϵ' and of the imaginary part ϵ'' of the complex permittivity $\epsilon_d^* = \epsilon' - j\epsilon_d''$, plotted vs. the frequency f for LiAsF_6 and LiClO_4 in DMC. The solid lines are the sum of two Debye single relaxation processes according to the functions

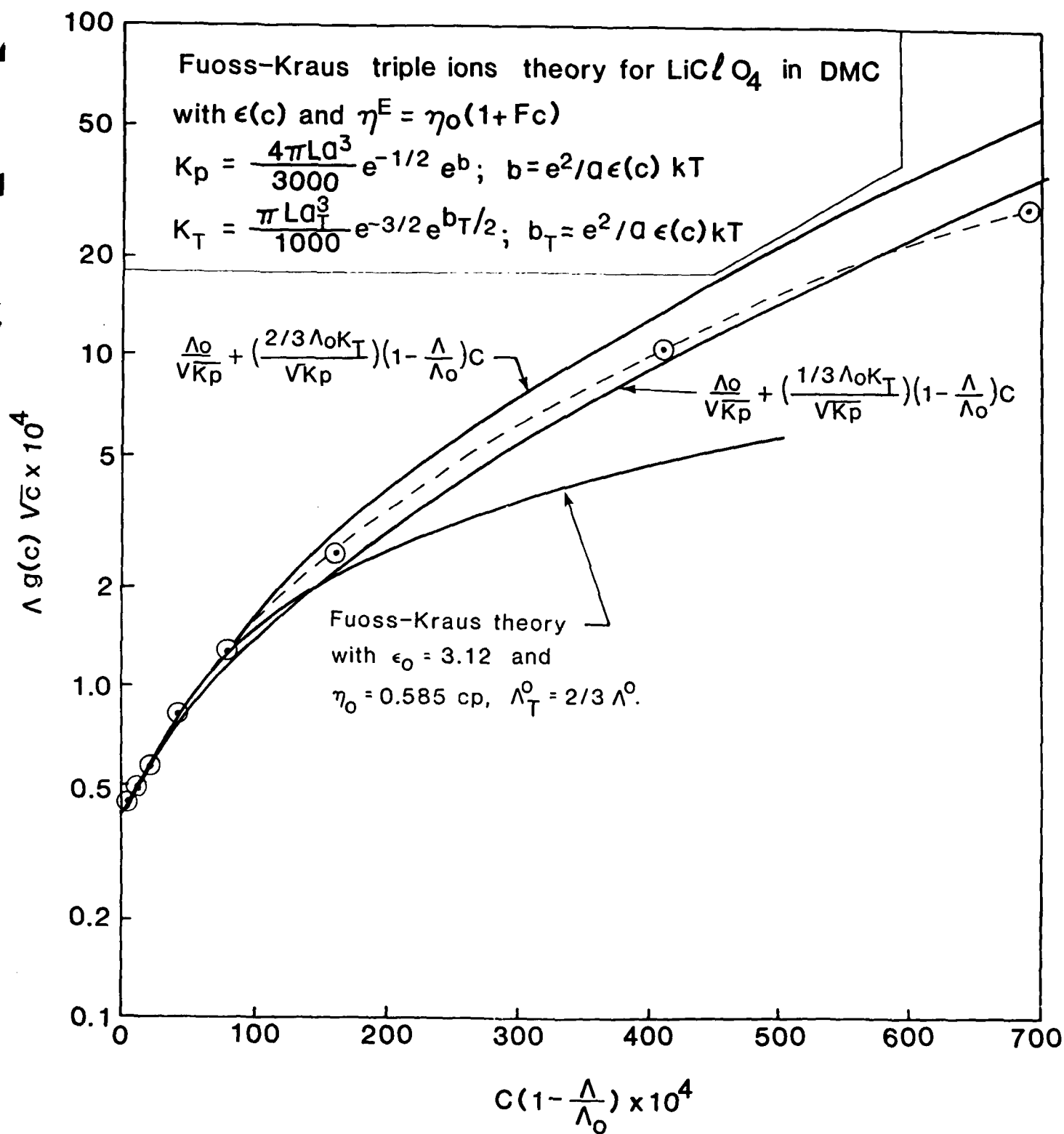
$$\epsilon' = \frac{\epsilon_o - \epsilon_{oo1}}{1 + (f/f_1)^2} + \frac{(\epsilon_{oo1} - \epsilon_{oo2})}{1 + (f/f_2)^2} + \epsilon_{oo2} \quad (\text{VI})$$

$$\epsilon_d'' = (\epsilon_o - \epsilon_{oo1}) \frac{f/f_1}{1 + (f/f_1)^2} + (\epsilon_{oo1} - \epsilon_{oo2}) \frac{f/f_2}{1 + (f/f_2)^2}$$

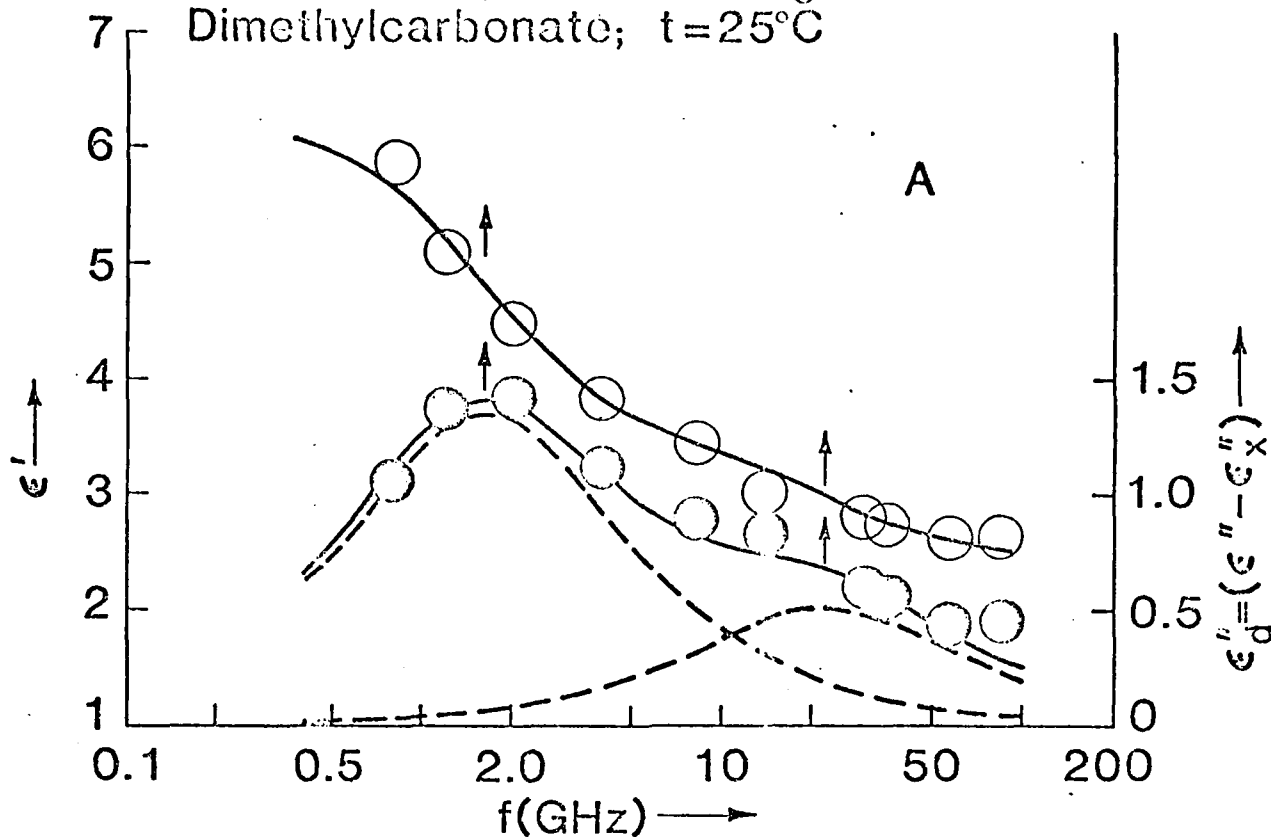
with $\epsilon_o, \epsilon_{oo1}, \epsilon_{oo2}, f_1, f_2$ relaxation parameters. ϵ_o is the static permittivity of the solution ($\epsilon_o - \epsilon_{oo}$) and $(\epsilon_{oo1} - \epsilon_{oo2})$ the respective relaxation strength of solute and solvent, f_1 and f_2 the relaxation frequencies associated with the solute and the solvent in the solution. ϵ_{oo1} should extrapolate at zero electrolyte concentration to the static permittivity of the pure solvent. In Figs. 7 and 8 the Cole-Cole plots of the quantities ϵ_d'' vs. ϵ' are also depicted. The solid lines correspond to the sum of two Debye processes according to Eqs. (VI). In the above, ϵ_d'' is the total dielectric loss ϵ'' subtracted of the contribution due to the conductance $\epsilon_x'' = 1.8 \times 10^{12} X / f$ with X the specific conductance of the solutions ($\Omega^{-1} \text{cm}^{-1}$). In Table II the dielectric relaxation parameters are reported together with the conductivity X . Eqs. (VI) have been fitted to the data by a trial and error procedure that minimize the summations $\sum |\Delta \epsilon'| + \sum |\Delta \epsilon''|$



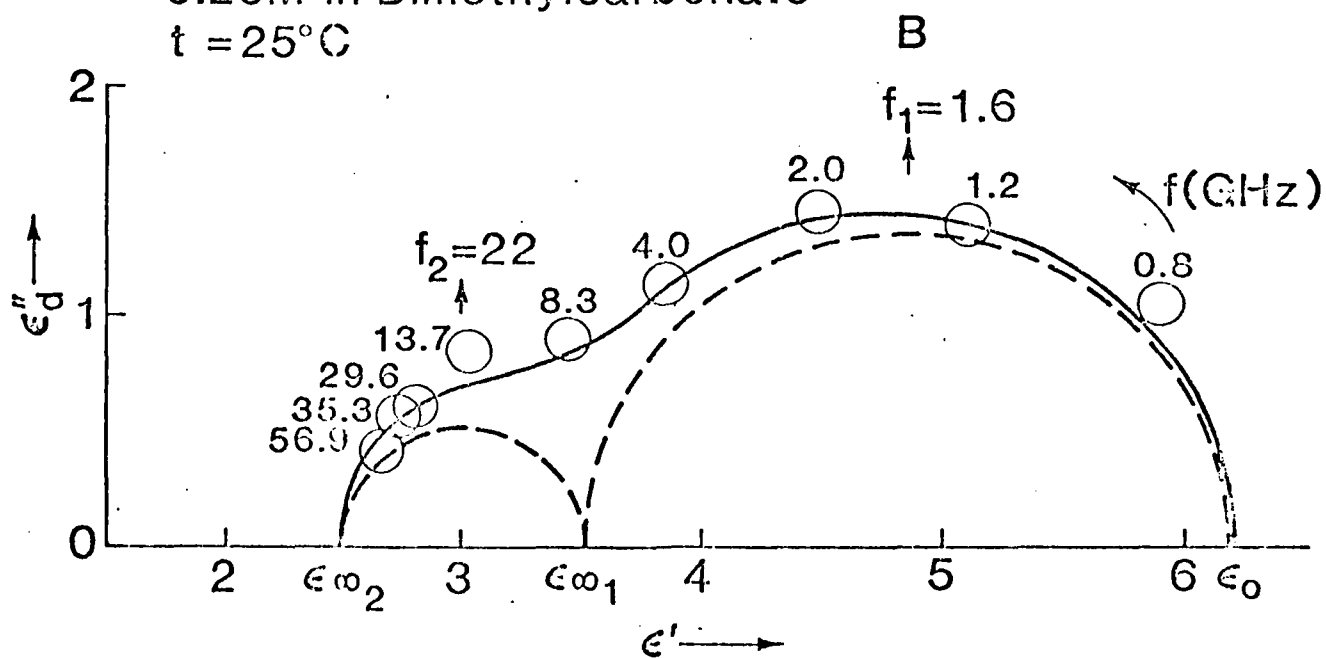


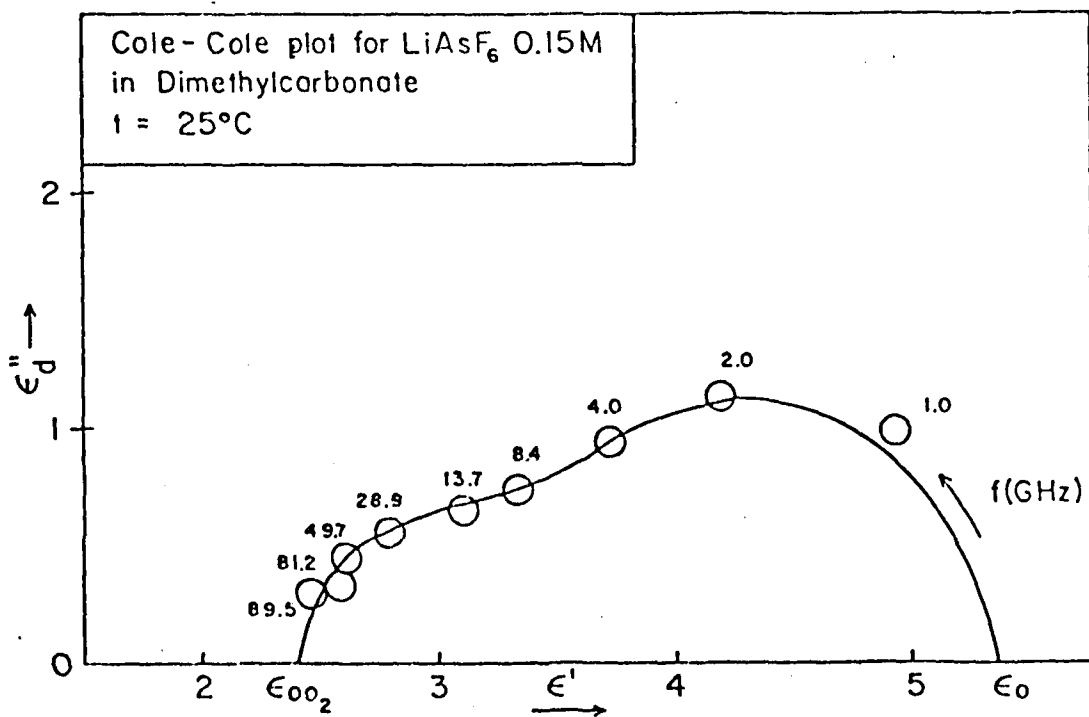
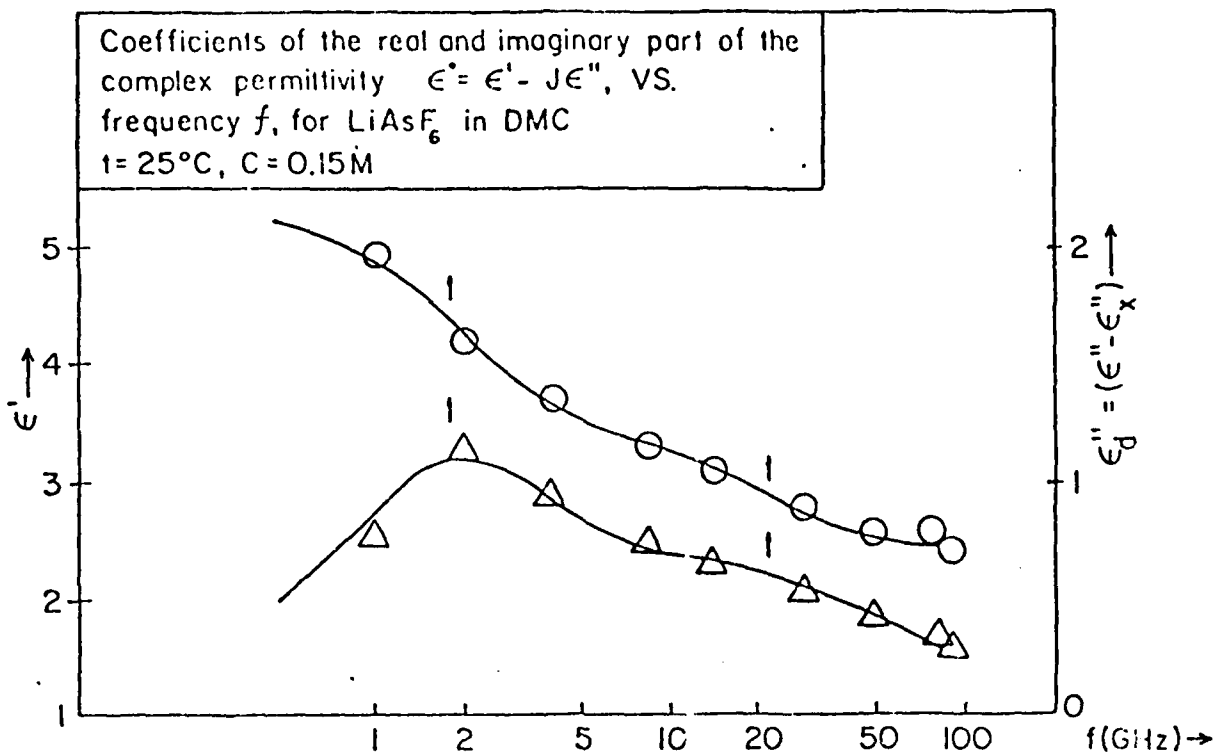


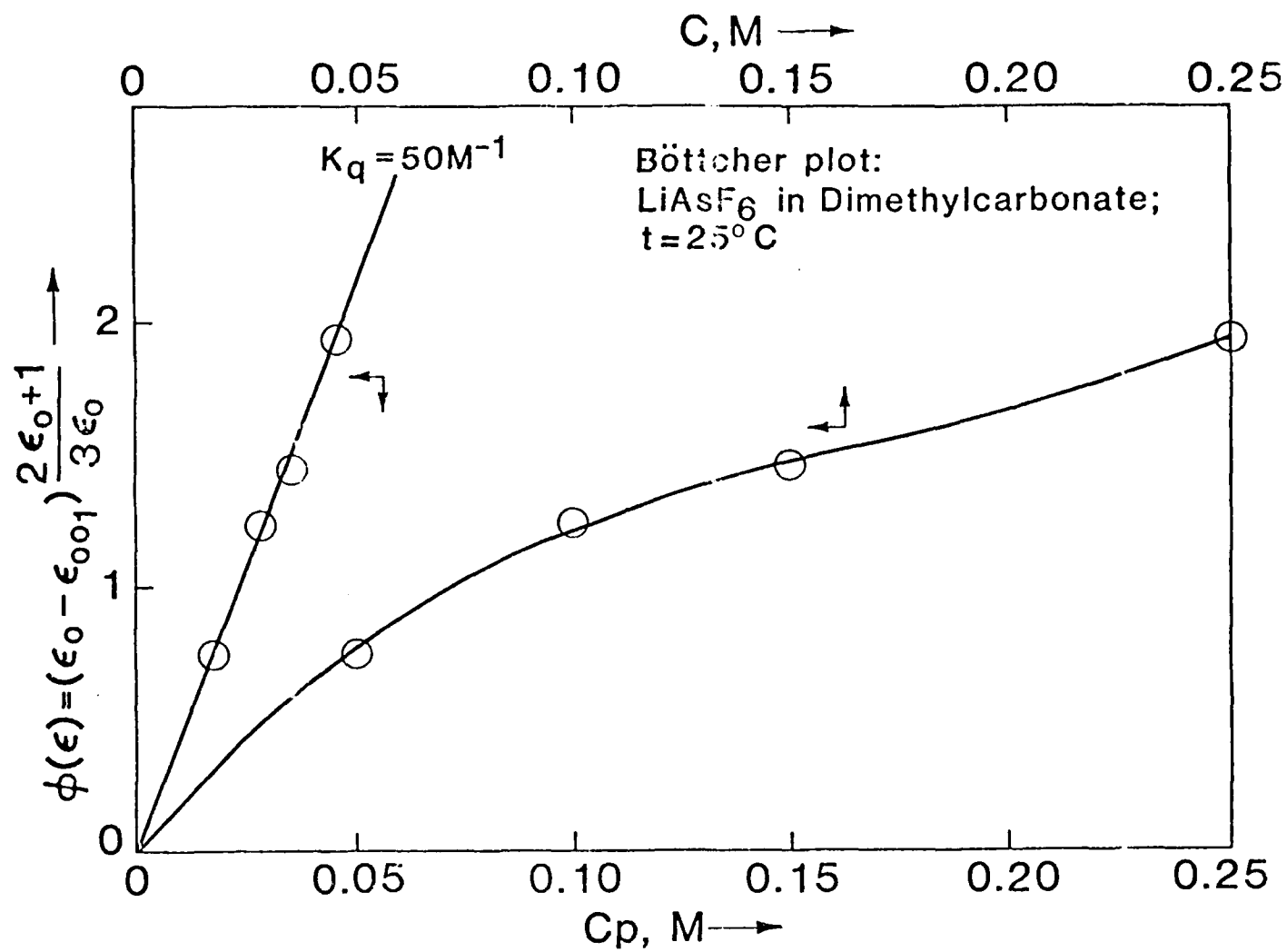
Components of the real and of the imaginary part of the complex permittivity $\epsilon^* = \epsilon' - j\epsilon''$ vs the frequency f , for LiAsF_6 0.25M in Dimethylcarbonate; $t = 25^\circ\text{C}$

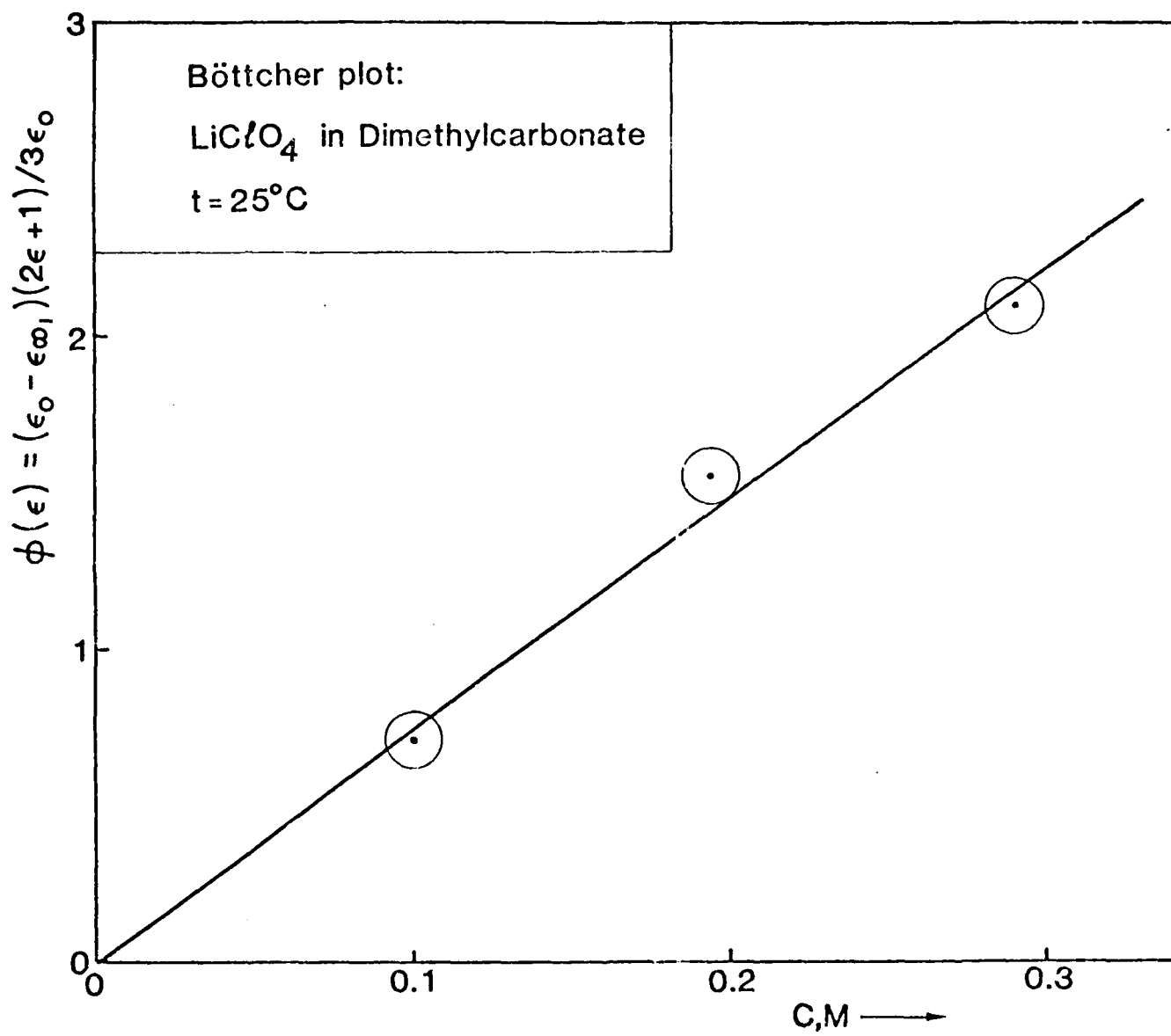


Cole - Cole plot for LiAsF_6 0.25M in Dimethylcarbonate
 $t = 25^\circ\text{C}$









END

FILMED

4-85

DTIC